Desalination and Water Treatment
www.deswater.com

doi: 10.5004/dwt.2019.23933

155 (2019) 237–249
July

Adsorption mechanism of Pb(II) and Ni(II) from aqueous solution by TiO_2 nanoparticles: kinetics, isotherms and thermodynamic studies

Shamshad Khan[a], Zhang Dan[a,*], He Haiyan[a,b]

[a]*Laboratory of Mountain Environmental Diversity and Control, Institute of Mountain Hazards and Environment, Chinese Academy of Sciences and Ministry of Water Conservancy, Chengdu 610041, China, Tel. +86 13708008342; Fax: +86 28 85222258; emails: daniezhang@imde.ac.cn (Z. Dan), shamshadkhan768@yahoo.com (S. Khan), 429602425@qq.com (H. Haiyan)*
[b]*University of Chinese Academy of Sciences, Beijing 100081, China*

Received 20 August 2018; Accepted 7 February 2019

ABSTRACT

In this work, TiO_2 nanoparticles (TNPs) were used as an absorbent to remove Pb(II) and Ni(II) from aqueous solution. The effect of pH, ionic strength (IS), humic acid (HA), contact time, foreign ions and temperature on the adsorption of Pb(II) and Ni(II) onto TNPs were examined by batch technique. The results showed that the adsorption of Pb(II) and Ni(II) was dominated by outer-sphere surface complexation at pH < 6.0, whereas, inner-sphere surface complexation was the main absorption mechanism at pH > 6.0. The maximum absorption capacity of Pb(II) and Ni(II) onto TNPs calculated from a Langmuir model was 40.00 and 26.32 mg g^{-1}, respectively at 303 K, exhibiting higher efficiency for Pb(II) absorption than Ni(II). The thermodynamic parameters ($\Delta H°$, $\Delta S°$ and $\Delta G°$) of Pb(II) and Ni(II) onto TNPs were calculated from the temperature dependent absorption, and their results demonstrated that absorption was endothermic and spontaneous. This analysis demonstrates that the TNPs can be utilized as an appropriate absorbent for the absorption of metal ions from solutions.

Keywords: Absorption; Ionic strength; TiO_2 nanoparticles; Heavy-metal ions removal

1. Introduction

Due to rapid growth of industrialization in the last centuries, an increase of heavy metal concentration in the environment has been observed. Among these heavy metals, Pb(II) and Ni(II) are some of the most widespread contaminants in the environment. They can be introduced to soil and water systems through mining, non-ferrous metal industry, metalworking and finishing processes, electroplating, electrical and electronics, printing and photographic [1–5]. Therefore, it is essential to find techniques to successfully remove heavy metals from wastewater or different industrial effluents before their release to the environment. Strict environmental protection regulations on the disposal of heavy metals and increasing demands for clean water with low levels of heavy metals make it deeply important to develop a variety of suitable techniques for heavy metals removal [6,7].

In order to remove effectively the heavy metal ions from water, several methods have been applied, including filtration, surface complexation, chemical precipitation, ion exchange, electrodeposition, absorption and membrane processing [8–11]. Considering the available techniques for the removal of metal ions from a solution, adsorption is one of the most widely used effective, efficient, and economic technique [3]. As a result, many researchers have observed the use of various types of adsorbent materials such as Nickel ferrite bearing nitrogen-doped mesoporous carbon [12], Ti(IV) iodovanadate cation exchanger [13], agricultural waste [14], Lycopersicumesculentum (tomato) leaf powder [15], ethylene diamine tetra acetic acid-Zr(IV) iodate composite

* Corresponding author.

cation exchange [16], tea waste [17], microorganism [18], yeast [19], sludge ash [20], date pits [21], and red mud [22]. Recently, TNP nanoparticles have also demonstrated high absorption efficiency for metal ion removal [3]. TNPs has large surface areas, well-defined pore sizes, high pore volume and high sorption ability, ease of modification, and diversity in surface modification [6]. Absorption into TNPs can give extraordinary chances for the removal of heavy metals in highly efficient and cost-effective approaches. TNPs are widely studied for its potential application in booming degradation and absorption of organic pollutants in the aqueous solution [23–25]. TNPs have been investigated as absorbent due to very favorable ligand adsorption behavior by inner-sphere complex formation [26]; whereas, Xu et al. [27] proposed it because of electrostatic interaction and *H* bonding between TNPs and organic polar groups. It was observed that p_y orbital of the oxygen atoms had the capacity to absorb the gaseous NO_2 on the TNPs surface [28]. The Na(I) within the TNP structure dominates the sorption potential of TNPs during the sorption of organic dyes on TNPs [29]. It was reported that TNPs demonstrated high absorption efficiency for metal ions due to the strengthening O–H bond and the intercalation of H(I) in TNP structure [30,31]. It was also observed, that the maximum absorption of Reactive Red 195 was 86.96 mg g^{-1} onto TNPs [32]. Janus et al. [33] reported that Direct Green 99 absorption increased to 96.77 mg g^{-1} into modified TiO_2 with carbon, which was greater than that of the bare TiO_2. Vu et al. [34] examined that the absorption ability of Cu(II) on TNPs prepared through electrospinning was about 12.8 mg g^{-1}. However, little consideration has been paid to the chemistry of Pb(II) and Ni(II) absorption mechanism onto TNPs.

Therefore, the objectives the present study are (1) to examine the absorption of Pb(II) and Ni(II) from aqueous solution onto TNPs with respect to various environmental parameters; (2) to assume the underlying mechanism of metal binding; (3) to estimate the thermodynamic parameters from temperature dependent adsorption isotherms and to intensely identify the absorption processes, and thus to examine the possible applications of TNPs as an absorbent in heavy metal contamination management.

2. Materials and methods

2.1. Materials

The analyzed TiO_2 nanoparticles (anatase form) and humic acid in this study were obtained from Sigma-Aldrich (Ankara, Turkey). The characteristics of the TiO_2 nanoparticles provided by the supplier are presented in Table 1. Humic acid (>99%) is black crystalline powder, which is selected as a NOM model molecular used in this study. The stock solutions of Pb(II) and Ni(II) were prepared by dissolving $Pb(NO_3)_2$ and $Ni(NO_3)_2$ in distilled water and then diluted to 60 mg L^{-1}, respectively. All other materials utilized in the experiments were obtained in analytical purity and used directly without any further purification. All the glassware was prewashed with 5% HNO_3 for 24 h, systematically rinsed with distilled water three times and dried at 60°C before use.

Table 1
Physiochemical properties of the studied TiO_2 nanoparticles (TNPs) adsorbent

Parameters	Value
Particle size	<25 nm
Appearance	White powder
Density	3.9 g cm^{-3}
Bulk density	0.04–0.06 g cm^{-3}
BET surface area	45–55 m^2 g^{-1}
Crystal form	Anatase

2.2. Materials characterization

The surface morphology of TNPs, before and after metal absorption, was determined by scanning electron microscope (Stereoscan 440, Leica). FTIR spectra of samples before and after absorption of Pb(II)/Ni(II) onto TiO_2 were recorded at room temperature (FTIR, Bruker Vertex 70). The pH_{ZPC} (zero point of charge) of TNPs is approximately 4.2 found by Zeta-sizer Nano S Instrument (Malvern Instrument Ltd, Malvern) as illustrated in detail in our earlier study [35] and Total Organic Carbon analyzer (Apollo 9000, Teledyne Tekmar), was used to determine the TOC content of HA (54.8 mg TOC L^{-1}), after centrifuging and filtering through disposable 0.45-μm membranes as illustrated in our previous work [3].

2.3. Absorption procedures

The absorption of Pb(II) and Ni(II) onto TNPs was carried out under ambient conditions by the batch method. The mixtures of the TNPs and $NaClO_4$ solutions were pre equilibrated for 24 h and then desired concentration of various components Pb(II) and Ni(II) were added. The pH of each solution was adjusted to the required value by the addition of $HClO_4$ or NaOH. After absorption experiments, the suspensions were centrifuged at 9,000 rpm for 30 min. The supernatant was hereafter used to determine the metal ion concentration in solution using a graphic furnace atomic absorption spectrometry (AA-600, Perkin- Elmer, USA). The absorption of Pb(II) and Ni(II) was determined by the following equation:

$$\text{Absorption } \% = \frac{C_0 - C_{eq}}{C_0} \times 100 \quad (1)$$

The absorption capacity, q_e (mg g^{-1}) was calculated according to the following equation:

$$q_e = \frac{(C_0 - C_e)V}{m} \quad (2)$$

where C_0 and C_e (mg L^{-1}) are the respective initial and final concentration of heavy metals in the solution phase; V is the volume of solution (L) and m (g) represents weight of adsorbent. All the experiments were repeated three times and average values were reported. The standard deviation was found less than 5%.

3. Results and discussion

3.1. Characterizations of TNPs

The FTIR analysis of TNPs, TNPs/Pb and TNPs/Ni was performed using a FTIR spectrometer as shown in Fig. 1(a). The FTIR spectra of heavy metal loaded TiO_2 revealed rather similar spectra to that of the unloaded TiO_2, all the samples displayed a broad band at around 460–700 cm^{-1}. This was due to the vibrational mode of the Ti-O-Ti and stretching mode of Ti-O [36]. The peak at approximately 3,422 cm^{-1} was attributed to the stretching vibrations of the O–H group and bands appearing at 1,635 cm^{-1} were the flexion vibrations of the O–H bond of absorbed water molecules [37]. The FTIR bands of all the samples at 1,384 cm^{-1} were attributed to NO_3, indicating that nitrogen atoms were incorporated in the TNPs [38]. The peaks at 1,051 and 1,124 cm^{-1} in the TiO_2-dispersion vanished or shifted to another position after the heavy metal absorption, resulted from the interactions between the hydroxyl groups and Pb(II)/Ni(II) existed.

Fig. 1(b)–(d) demonstrates the SEM micrographs of the sample TNPs before and after metal absorption, respectively. The images expose that TNPs powered consist of 0.2–1.0 μm spherical large particles. TNPs form the large particles due to their tendency towards aggregation or agglomeration. Similar results were illustrated in the work of Bakardijieva et al. [39], in which the large (1–2) spherical particles shown in the SEM images shown to consist of 4–5 nm TiO_2 nanoparticles interlayered by small fractions of amorphous materials in the TEM analysis. However, the TNPs (Fig. 1(b)) had a rough surface with heterogeneous holes and pores that generate a large surface area which showed that metals can be absorbed into its surface. Figs. 1(c) and (d) demonstrate micrographs of the TNPs surface after absorbed Pb(II) and Ni(II), the surface of TNPs was relatively less porous because of the formation of a layer over the absorbent surface after absorption of Pb(II) and Ni(II).

3.2. Influence of solution pH and ionic strength

The pH value of the solution plays a significant role on the sorption of Pb(II) and Ni(II) onto TNPs and is illustrated in Figs. 2(a) and (b). The absorption of Pb(II), gradually increases with an increase in pH ranging from 2.4–5.0, then maintains a high level at pH 5.0–10.0. About 98% of Pb(II) is absorbed at pH 6.0, whereas the considerably decreased absorption of Pb(II) onto TNPs is recorded at pH above 10.0. Absorption of Ni(II), slowly increases with pH ranging from 2.0–4.0, then pH range abruptly increase, from 4.0 to 6.0, and finally sustains with a level of higher than 6.0 pH. Approximately, 60% of Ni(II), is absorbed onto TNPs at pH higher than 6.0. The point of zero charge (pH_{pzc}), value of TNPs is about 4.2 [35].

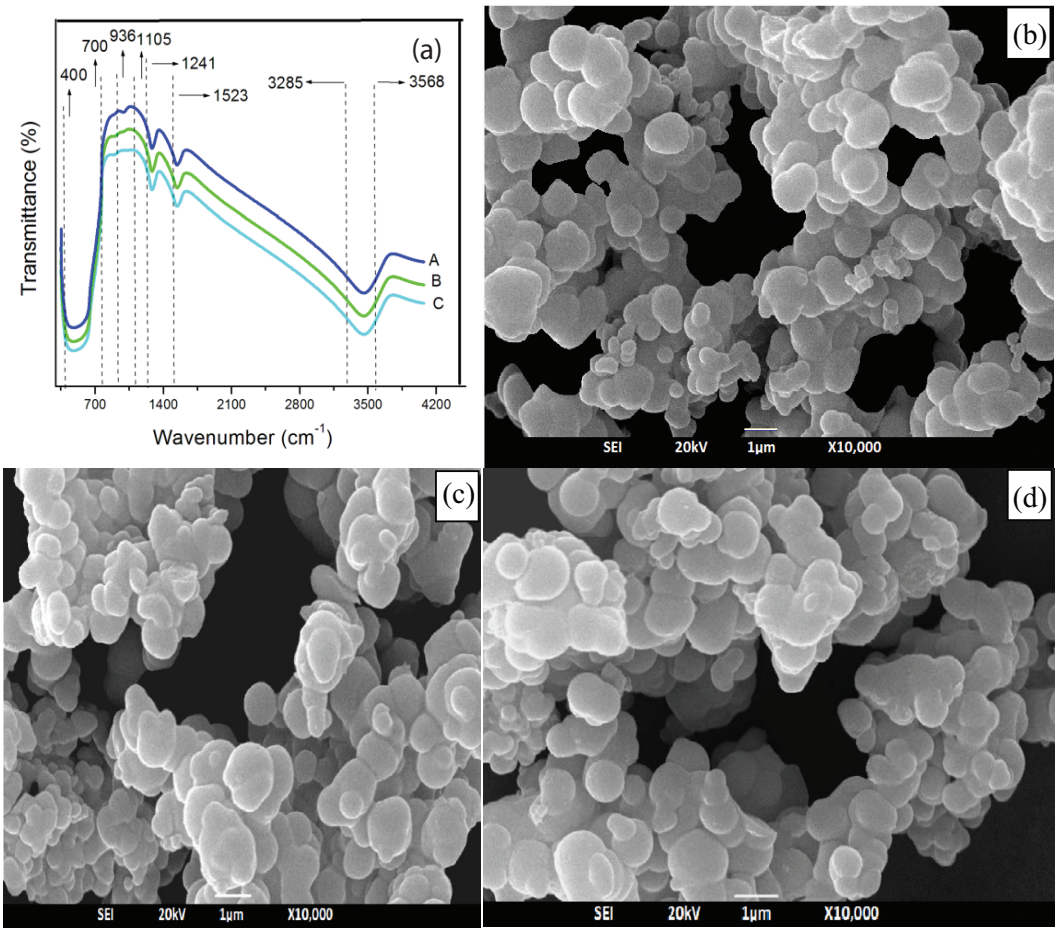

Fig. 1. FTIR spectra of (a): TNPs (A) TNPs-Pb(II) (B) TNPs-Ni(II) (C) and SEM images of TNPs (b); TNPs-Pb(II) (c); TNPs-Ni(II) (d).

At pH < pH_{pzc}, the surface charge of the TNPs is positive, whereas the surface of TNPs is negatively charged at pH > pH_{pzc}. It is recognized that the Pb(II) and Ni(II) species are significant to Pb(II) and Ni(II) absorption. Figs. 2(c) and (d) illustrate the distribution of Pb(II) and Ni(II), species as a function of pH by using the hydrolysis constants of Pb(II) and Ni(II), given in Table 2 [40,41].

Fig. 2(c) illustrates that Pb(II) exists in the species of Pb^{2+}, $Pb(OH)^{+}$ $Pb(OH)_2^{0}$ and $Pb(OH)_3^{-}$ at various pH values. The predominant lead species are Pb^{2+} at pH < 6.0, $Pb(OH)^{+}$ at pH 7.0–9.0, $Pb(OH)_2^{0}$ at pH 9.0–11.0 and $Pb(OH)_3^{-}$ at pH > 11.0, respectively. While the predominant nickel species are Ni^{2+} at pH < 8.0, $Ni(OH)^{+}$ at pH 9.0–10.0, $Ni(OH)_2^{0}$ at pH 10.0–11.0 and $Ni(OH)_3^{-}$ at pH > 11.0, respectively (Fig.1(d)). As a result, the Pb(II) and Ni(II) absorption at low pH can result in protonation reaction on the surface of TNPs and the concentration of protonated sites ($\equiv TiOH_2^{+}$) decreases with increasing pH. The expression can be express as follows:

$$TiOH + H^{+} \Leftrightarrow TiOH_2^{+} \quad (3)$$

$$TiOH \Leftrightarrow TiO^{-} + H^{+} \quad (4)$$

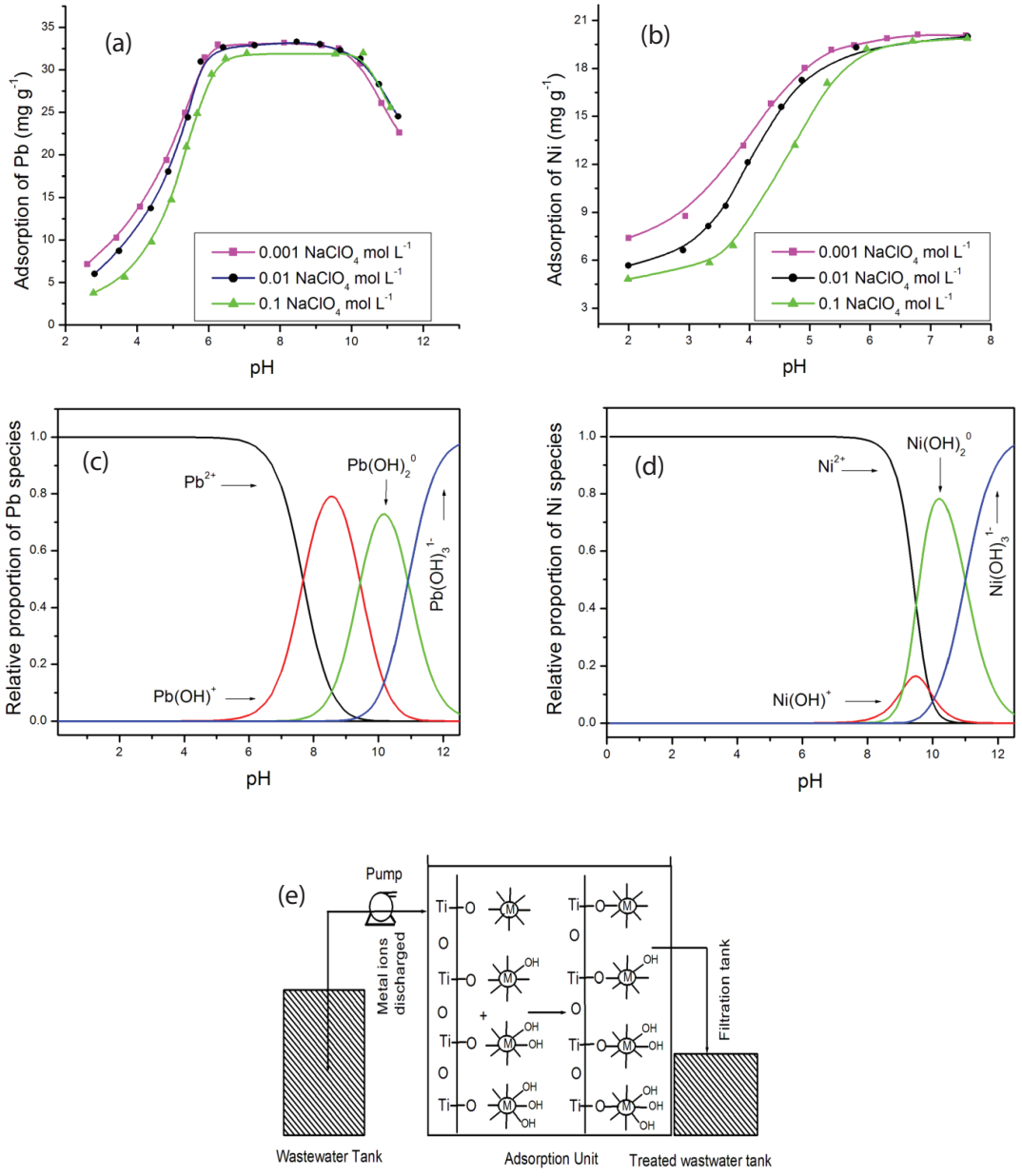

Fig. 2. Effect of ionic strength on Pb(II) and Ni(II) adsorption onto TNPs as a function of pH (a and b); relative proportion of Pb(II) and Ni(II) species as a function of pH (c and d); Possible adsorption scheme for metal ions onto TNPs (e). [Adsorption conditions: adsorbent dosage = 300 mg L^{-1}, pH = 5.4, initial concentration of Pb(II)/Ni(II) = 10 mg L^{-1} and temperature = 303 K].

Table 2
Equilibrium constants of Pb(II) and Ni hydrolysis reactions

Hydrolysis reactions of Pb(II)	log*K*	Hydrolysis reactions of Ni(II)	log*K*
$Pb^{2+} + H_2O \Leftrightarrow Pb(OH)^+ + H^+$	−7.68	$Ni^{2+} + H_2O \Leftrightarrow Ni(OH)^+ + H^+$	−9.90
$Pb^{2+} + 2H_2O \Leftrightarrow Pb(OH)_2^0 + 2H^+$	−17.12	$Ni^{2+} + 2H_2O \Leftrightarrow Ni(OH)_2^0 + 2H^+$	−19.00
$Pb^{2+} + 3H_2O \Leftrightarrow Pb(OH)_3^- + 3H^+$	−28.03	$Ni^{2+} + 3H_2O \Leftrightarrow Ni(OH)_3^- + 3H^+$	−30.00

where $TiOH_2^+$, TiOH and TiO^- are positive, neutral, and negative hydroxyl groups surface, respectively. It was observed that cationic soluble TNPs complexes in acid solutions are in the form of $TiOH_2^+$ [42]. The binding of Pb(II) and Ni(II) by surface functional groups starts at pH_{pzc} and increases sharply with increasing pH. The reaction of Pb(II) and Ni(II) (referred as M^{2+}) ions with TNPs involves bond configuration of surface complexes with metal ions (M^{2+}) are given in the following chemical equations:

$$TiOH + M^{2+} \Leftrightarrow TiOM^+ + H^+ \quad (5)$$

$$Ti - OH(OH)_2 + M^{2+} \Leftrightarrow Ti - (OH_2)O - M^+ + H^+ \quad (6)$$

Therefore, the Pb^{2+} and Ni^{2+}absorption is difficult because of coulombic repulsion below the pH_{zpc} (4.2). Thus, the formation of complex between Pb(II)/Ni(II) and the TNPs surface proposes an inner-sphere. However, at high pH range 4.2–6.0, the concentration of deprotonated sites (≡TiO–) increases with an increase in pH due to the surface deprotonation reaction as shown in Eq. 6. The deprotonated sites are more accessible to maintain Pb(II) and Ni(II) ions and surface complexation between Pb^{2+}, Ni^{2+}, $Pb(OH)^+$, $Ni(OH)^+$ and TNPs is facilitated, therefore resulting in accurate increase of Pb(II) and Ni(II) absorption at pH 4.2–6.0. However, absorption of Pb(II) onto TNPs is reduced because of opposite charges between the TNPs surface and Pb(II) species such as $Pb(OH)_3^-$ species at higher pH (pH > 10.0). The formation of surface metal complexes can also be shown conceptually by the following scheme (Fig. 2(e)). The sorption of species on the surface of OH^- such as TNPs occurs through the formation of O–M bonding [43]. The absorbed metal species can go through hydrolysis reaction as pH increases. This gives a series of metal surface complexes such as TiO^- MOH^+, TiO–$M(OH)_2$ and TiO–$M(OH)_3^-$species.

Figs. 2(a) and (b) show the absorption of Pb(II) and Ni(II) onto TNPs as a function of pH in 0.001, 0.01 and 0.1 mol L^{-1} $NaClO_4$ solutions, respectively. From the figures it is observed that the Pb(II) and Ni(II) absorption onto TNPs is affected by IS at pH < 6.0. No significant difference of Pb(II) and Ni(II) absorption is observed in the three various concentrations of $NaClO_4$ at pH > 6.0. The influence of IS on Pb(II) and Ni(II) absorption is similar with those reported in the literatures [44,45]. The result of the present study illustrates that Pb(II) and Ni(II) can form a β-plane complex reaction at low pH values, as the absorption is significantly influenced by the β-plane complex reaction of the electrolyte on the view of modified triple-layer complex model as explained by Wu et al.[46]. Meanwhile, Pb(II) and Ni(II) can form an *o*-plane complex reaction at high pH values without being influenced by the β-plane complex reaction of the electrolyte. Therefore, in this view, the pH and ionic strength-dependent Pb(II) and Ni(II) absorption proposes that the Pb(II) and Ni(II) absorption onto TNPs is predominated by outer-sphere surface complexation at pH < 6.0. While the absorption of Pb(II) and Ni(II) is generally due to inner-sphere surface complexation at a range of pH 6–10 and pH > 6.0, respectively.

3.3. Influence of cation

In order to estimate the effect of cations on Pb(II) and Ni(II) absorption, the pH-dependent absorption of Pb(II) and Ni(II) onto TNPs is examined in 0.01 mol L^{-1} $LiClO_4$, $NaClO_4$ and $KClO_4$ solutions, respectively (Fig. 3). The influence of cations on the absorption of Pb(II) and Ni(II) onto TNPs at lower pH (pH < 6.0) shows that the effect of K^+ on Pb(II) and Ni(II) absorption is larger than the Li^+ and Na^+. Thus, the absorption of Pb(II) and Ni(II) is highest in $LiClO_4$ and is lowest in $KClO_4$, illustrating that cations can modify the surface properties of TNPs and thus influence the absorption of Pb(II) and Ni(II) onto TNPs. The impact of cations on Pb(II) and Ni(II) absorption can also be verified by the radius 2.32 A°, 2.76 A° and 3.40 A° of the K^+, Na^+ and Li^+, respectively [47]. The smaller the radius of K^+ is larger the effect on the Pb(II) and Ni(II) absorption than those of Na^+ and Li^+. At pH > 6.0, no significant distinction of Pb(II) and Ni(II) absorption to TNPs in $LiClO_4$, $NaClO_4$ and $KClO_4$ solutions is found, which may be ascribed to the inner-sphere surface complexation or surface precipitates at high pH values as mentioned in the previous section. Li et al. [48] studied the influence of Li^+, Na^+ and K^+ on the absorption of Cu(II) on GMZ bentonite, and observed that at pH < 7, the absorption of Cu(II) on GMZ bentonite was the highest in Li^+ cation solution and the lowest in K^+ cation solution. Hu et al. [49] also achieved the similar results by the influence of cation ions (Li^+, Na^+ and K^+) on the absorption of Ni(II) in goethite and illite, respectively.

3.4. Influence of anion

In order to investigate the influence of anions on the absorption of Pb(II) and Ni(II), the absorption of Pb(II) and Ni(II) onto TNPs was examined in 0.01 mol L^{-1} $NaClO_4$, $NaNO_3$ and NaCl solutions, respectively. The influence of anion ions (ClO_4^-, NO_3^-, and Cl^-) on the absorption of Pb(II) and Ni(II) onto TNPs is shown in Fig. 4. At pH < 6.0, the anions clearly affect Pb(II) and Ni(II) absorption onto TNPs. It was observed under the same pH ranges that the absorption of Pb(II) and Ni(II) onto TNPs in a NaCl solution is lower than in a $NaNO_3$ solution and highest in a $NaClO_4$ solution. This process could be explained by two aspects: (i) Pb(II) and Ni(II) can form soluble complex with inorganic acid radicals, because the inorganic acid radius of Cl^- is smaller than that of NO_3^- [47,50], Pb(II)/Ni(II) has higher attraction to Cl^- and a

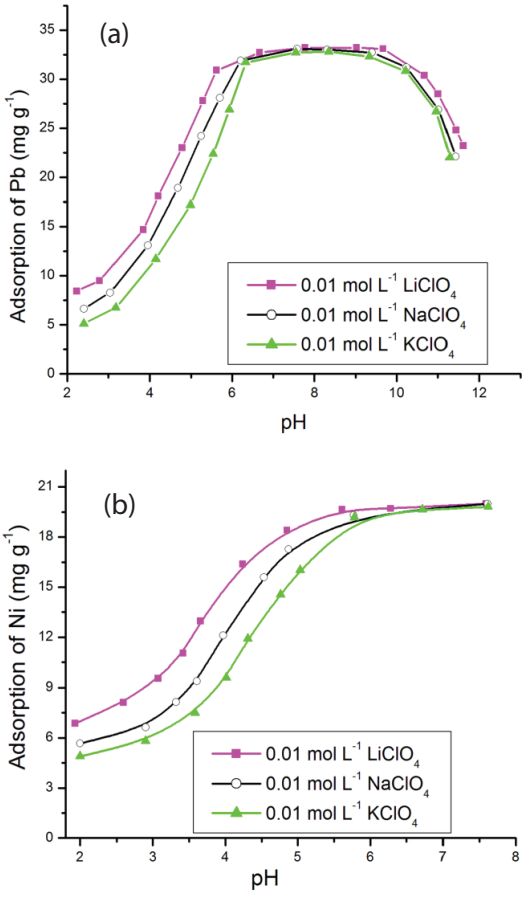

Fig. 3. Effect of cations on Pb(II) and Ni(II) adsorption onto TNPs as a function of pH (a and b). [Adsorption conditions: adsorbent dosage = 300 mg L^{-1}, pH 5.4, initial concentration of Pb(II)/Ni(II) = 10 mg L^{-1} and temperature = 303 K].

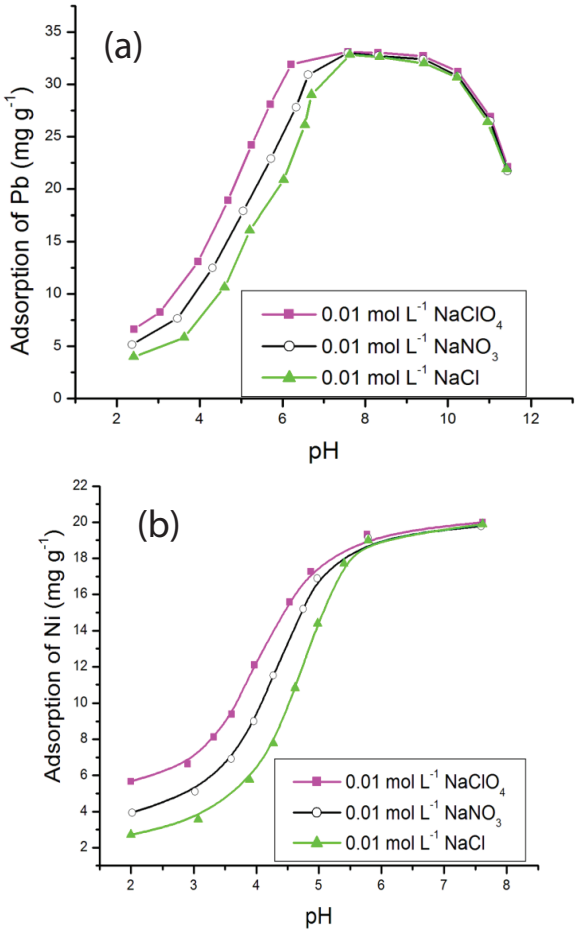

Fig. 4. Effect of anions on Pb(II) and Ni(II) adsorption onto TNPs as a function of pH (a and b). [Adsorption conditions: adsorbent dosage = 300 mg L^{-1}, pH 5.4, initial concentration of Pb(II)/Ni(II) = 10 mg L^{-1} and temperature = 303 K].

higher inclination for complexation with Cl^- relative to NO_3^-, leading to a stronger reduction of Pb(II)/Ni(II) concentration (ii) Cl^{-1} absorbed on the surface of TNP through idiocratic absorption which is a little bit easier absorption than that of other anions (NO_3^- and ClO_4^-), and Cl^- absorption into TNP surface changes the surface characterizes of TNPs and reduces the accessibility of binding sites for Pb(II) and Ni(II). The smaller inorganic acid radicals ($Cl^- < NO_3^- < ClO_4^-$) can take up more ionic exchange sites and lead to decrease the Pb(II) and Ni(II) sorption onto TNPs [47,50].

3.5. Influence of humic acid

Humic acid (HA) has been commonly used as a representative of NOM that simulates the effect of NOM on numerous heavy metals absorption [51,52]. Fig. 5 shows pH dependent Pb(II) and Ni(II) absorption onto TNPs in the presence of HA. From the figure the absorption of Pb(II) and Ni(II) onto TNPs is observed to increase with the presence of HA at pH < 5.0 and pH < 6.0, respectively, whereas the absorption is reduced at pH > 6.0 and pH > 7.0, respectively. Zeta potential of HA is negatively charged in the pH range of 3.0–10.0 as determined by Ghosh et al. [53] and Yang et al. [54]. Thus the HA negative charged can be mostly absorbed by the TNPs at low pH range, consequently the strong complexation capacity of surface absorbed HA with Pb(II) and Ni(II) should consequence in the sorption of Pb(II) and Ni(II) onto TNP surface increasing at pH < 5.0 and pH < 6.0, respectively. Conversely, the negatively charged HA absorption of the on surfaces of negatively TNPs becomes complicated due to the electrostatic repulsion at high pH ranges. Therefore, the HA in solution forms soluble complexes of HA–Pb(II)/Ni(II) in solution, and thus decreases Pb(II) and Ni(II) absorption to TNPs.

3.6. Absorption kinetics

Kinetic behavior was significant to the sorption process because it illustrated the sorption rate of Pb(II) and Ni(II), and controlled the residual time of the entire sorption process. The absorption of Pb(II) and Ni(II) onto TNPs increases abruptly in the first 6 h, then high level absorptions are observed. About 73% and 60% of Pb(II) and Ni(II) is absorbed by TNPs, respectively, demonstrates that Pb(II) shows a higher absorption performance than Ni(II) absorption. It is found that 24 h is sufficient to achieve the absorption equilibrium.

In order to investigate the mechanisms of Pb(II) and Ni(II) absorption process, two kinetic models pseudo-first-order and pseudo-second-order were applied. These models are illustrated using the following equation:

$$\log\left(q_e - q_t\right) = \log q_e - \frac{k_1}{2.303}t \tag{7}$$

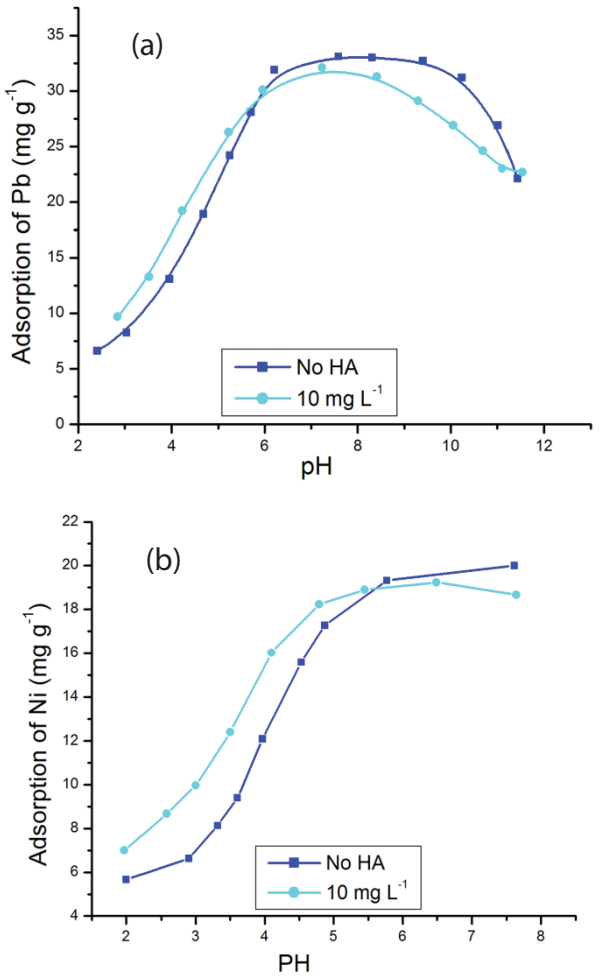

Fig. 5. Effect of HA on Pb(II) and Ni(II) adsorption onto TNPs as a function of pH (a and b). [Adsorption conditions: adsorbent dosage = 300 mg L^{-1}, pH 5.4, initial concentration of Pb(II)/Ni(II) = 10 mg L^{-1}, 0.01 mol L^{-1} $NaClO_4$ and temperature = 303 K].

$$\frac{t}{q_t} = \frac{1}{k_2 q_e^2} + \frac{1}{q_e}t \tag{8}$$

where q_t (mg g^{-1}) is the absorption at time t (min); q_e (mg g^{-1}) is the absorption capacity at absorption equilibrium; and k_1 (min^{-1}) and k_2 (g (mg $min)^{-1}$) are the rate constants for the pseudo-first-order and the pseudo-second-order models, respectively.

The calculated parameters of the two kinetic models are presented in Table 3. It was examined that the correlation coefficients (r^2) values for the pseudo-first-order kinetics are not satisfactory and the absorption capacities calculated by the model did not match the results from the experiments. This explains, that the pseudo-first-order kinetics is insufficient to show the absorption of Pb(II) and Ni(II) onto TNPs (Figs. 6(a) and (b)). For the pseudo second-order kinetics, the determined correlation coefficient (r^2) was high (>0.98), and the absorption capacities calculated by the model are in accordance to those determined by experiments. It verified that the Pb(II) and Ni(II) absorption ability was proportional to the number of active sites occupied onto TNPs. As the absorption process continued, active absorption sites would decrease. Thus, the rate of the Pb(II) and Ni(II) absorption onto TNPs normally depended on the accessible absorption sites on TNPs for Pb(II) and Ni(II) at any time.

3.7. Adsorption isotherms

The absorption isotherms of Pb(II) and Ni(II) onto TNPs at different temperatures are demonstrated in Figs. 6(c) and (d). The absorption of Pb(II) and Ni(II) are the highest at 333 K and lowest at 303 K, which shows that high temperature is favorable for Pb(II) and Ni(II) absorption onto TNPs. The Pb(II) and Ni(II), absorption at different temperatures were examined by the Langmuir model and the Freundlich model, which are given in the following equations:

$$\log q_e = \log k_F + \frac{1}{n}\log C_e \tag{9}$$

$$\frac{C_e}{q_e} = \frac{C_e}{q_m} + \frac{1}{q_m K_1} \tag{10}$$

where q_m is the amount absorbed in (mg g^{-1}), C_e is the equilibrium concentration (mg L^{-1}), K_F is the Freundlich constant indicating sorption ability and $1/n$ is the empirical constant representing sorption intensity. The absorption

Table 3
Pseudo-first-order and pseudo-second-order kinetic model constants of Pb(II) and Ni(II) adsorption onto TNPs

Fitting model	Metal	q_e (mg g^{-1}), exp	q_e (mg g^{-1}), cal	K^1(h^{-1})	r^2
Pseudo-1st-order model	Pb(II)	24.408	7.853	0.334	0.788
	Ni(II)	19.317	2.173	0.256	0.564
Pseudo-2nd-order model		q_e (mg g^{-1}), exp		K_2 (g(mg h)$^{-1}$)	r^2
	Pb(II)	24.408	25.00	0.062	0.999
	Ni(II)	19.317	20.00	0.076	0.998

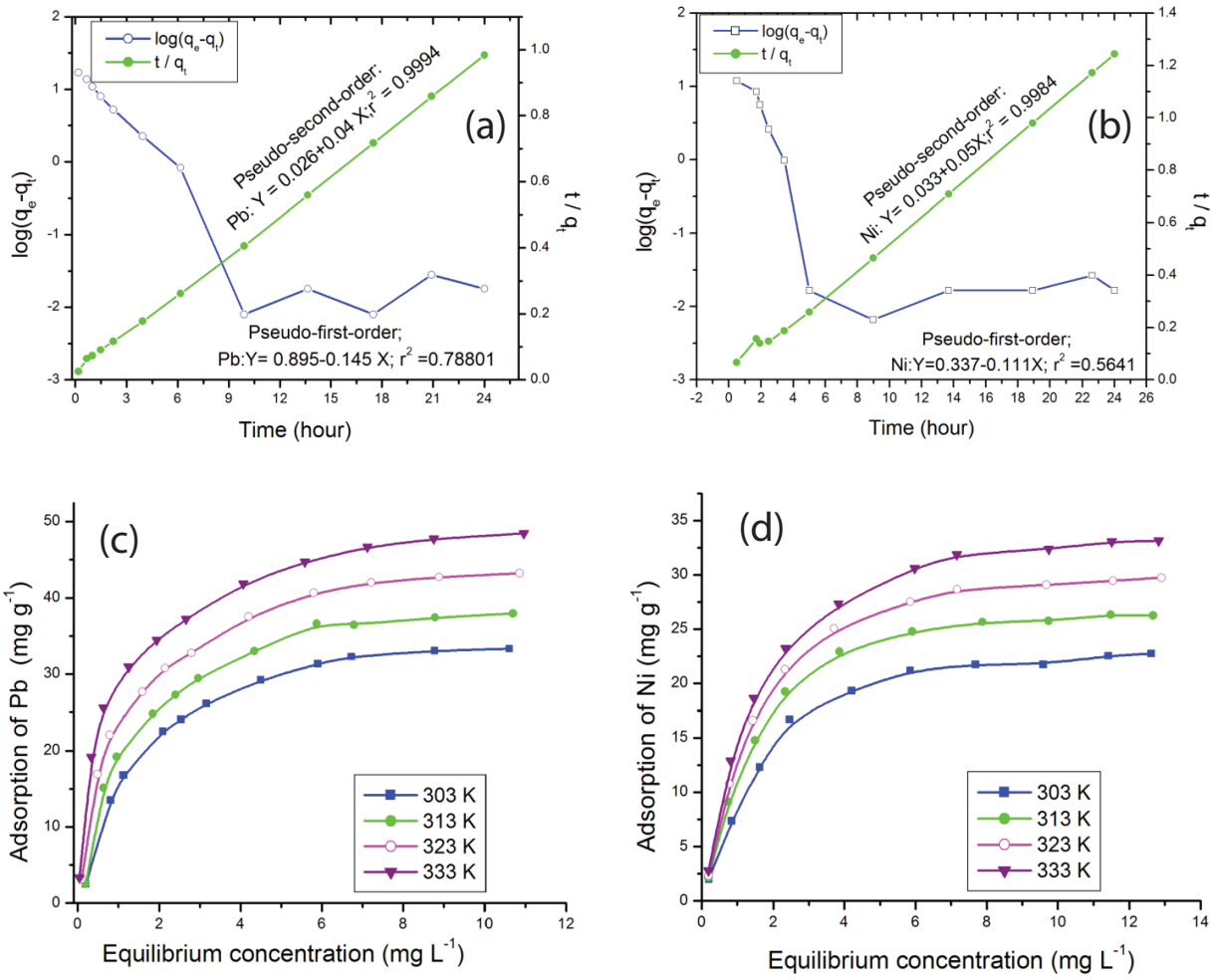

Fig. 6. Adsorption capacity of Pb(II) and Ni(II) onto TNPs; the fitting of different kinetic models for Pb(II) and Ni(II) adsorption onto TNPs; pseudo-first-order and pseudo-second-order of Pb(II) and Ni(II) (a and b); Adsorption isotherms of Pb(II) and Ni(II) on TNPs under the different temperature (c and d). [Adsorption conditions: adsorbent dosage = 300 mg L^{-1}, pH 5.4 and temperature = 303 K].

isotherms are exposed in Figs. 6(c) and (d) and the relative values achieved from the model are provided in Table 4. It is observed that the Langmuir model fits well for the Pb(II) and Ni(II), absorption isotherm as it gives the highest correlation coefficient value than the other isotherm model, indicating that monolayer surface absorption mechanism may exist.

Based on the Langmuir isotherm model, the calculated maximum absorption ability of absorbent (q_m) was observed to be 40.00, 45.45, 47.62 and 52.63 mg g^{-1} for Pb(II) and 26.32, 30.30, 34.48, and 38.46 mg g^{-1} for Ni(II) at 303, 313, 323 and 333 K, respectively. The high absorption ability of Pb(II), shown by TNPs may be elucidated by strong inclination of specific absorption due to electronegativity and electrostatics differences. Such similar results were found by Poursani et al. [55], they narrated that the sorption ability of heavy metals for nano- γ-Al_2O_3 nanoparticles on basis of Langmuir model followed such a sequence: Cr (13.89 mg g^{-1}) > Pb (7.39 mg g^{-1}) > Ni (0.04 mg g^{-1}). To estimate the absorption capacity of the TNPs absorbent, a comparative assessment (Table 5) was conducted between TNPs and several other absorbent materials reported in the literature. It was observed, that the TNPs used in this study possessed a higher Pb(II) and Ni(II), absorption capacity than most of the absorbents reported in the literature which can be due to its high active surface area of TNPs absorbent in the absorption of Pb(II) and Ni(II).

3.8. Adsorption thermodynamics

The thermodynamic parameters for the absorption of Pb(II) and Ni(II), onto TNPs can be calculated from the temperature-dependent absorption isotherms, which were performed at temperatures ranging from 303 to 333 K (Figs. 5(c) and (d)). The absorption of metal ions onto TNPs, increased as the temperature rose from 303 to 333 K as shown in Figs. 5(c) and (d). This shows, that the process is endothermic in nature. The thermodynamic parameters, ($\Delta H°$, $\Delta S°$ and $\Delta G°$) for the Pb(II) and Ni(II),absorption of onto TNPs can be calculated from the temperature-dependent absorption isotherms, (Fig. S1). The value of standard free energy change ($\Delta G°$) is calculated from the relationship [66]:

$$\Delta G° = -RT\ln K_0 \quad (11)$$

Table 4
Predicted isothermal constants of Pb(II) and Ni(II) by Freundlich and Langmuir isotherms at different temperatures

Model type	Metal	Temperature (K)	K_F (mg g^{-1}.(L mg^{-1})$^{-1}$)	1/*n*	r^2
Freundlich adsorption	Pb(II)	303	0.591	11.429	0.860
	Ni(II)	303	7.211	0.553	0.900
			q_m (mg g^{-1})	K_L (L mg^{-1})	r^2
Langmuir adsorption	Pb(II)	303	40.00	0.5435	0.984
		313	45.454	0.564	0.972
		323	47.619	0.875	0.998
		333	52.632	1.267	0.998
	Ni(II)	303	26.316	0.535	0.994
		313	30.303	0.589	0.993
		323	34.483	0.580	0.993
		333	38.461	0.591	0.995

Table 5
Comparison of maximum Pb(II) and Ni(II) monolayer adsorption capacities of various adsorbents

Adsorbent	Pb(II) adsorption capacity (mg g–1)	Ni(II) adsorption capacity (mg g–1)	References
TiO_2 nanoparticles	40.00	26.32	This study
Al_2O_3 modified with NOM		15.38	[3]
Ti(IV) iodovanadate cation exchange	18.80		[13]
Fe nanoparticles loaded ash (nFe-A)	833.33		[14]
Lycopersicum esculentum leaves powder		47.61	[15]
EDTA-Zr(IV) iodate composite cation exchanger	26.04		[16]
Polyaniline Sn(IV) tungstomolybdate nanocomposite	44.64		[56]
Sawdust activated carbon (FSAC)	80.64		[57]
Nano-composite adsorbent	173.6		[58]
Sodium dodecyl sulfate acrylamide Zr(IV) selenite (SDS-AZS)	18.38		[59]
Iron oxide modified with sewage sludge		7.80	[60]
Lignin		6.00	[61]
Activated sludge		8.80	[62]
Waste tea		18.40	[63]
Thuja orientalis (cone)		12.40	[64]
Al_2O_3 modified with walnut shells		6.80	[65]

where *T*(K) is the absolute temperature, *R* (8.314 J mol^{-1} K^{-1}) is the gas constant and K_0 is absorption distribution coefficient and was calculated from the slope of the plot ln q_e/C_e vs. q_e at different temperatures and extrapolating to zero q_e according to the technique recommended by Khan and Singh [67]. The values of $\Delta S°$ and $\Delta H°$ were determined from the slope and intercept of the plot of $\Delta G°$ vs. *T* by the following expression:

$$\Delta G° = \Delta H° - T\Delta S° \quad (12)$$

where $\Delta S°$ is the standard entropy change (J $(mol\ K)^{-1}$) and $\Delta H°$ is the standard enthalpy change ($kJmol^{-1}$). The positive $\Delta H°$ values for both metal ions shows that the absorption is endothermic in nature. The positive value of $\Delta S°$ reveals an irregular increase in the randomness in the system solic/solution interface throughout the absorption process while low values of $\Delta S°$ demonstrates that no notable changes occur to entropy. The negative $\Delta G°$ value confirms that the absorption process is spontaneous in nature (Table 6). The value of $\Delta G°$ becomes more negative with increase of temperature, which indicates more capable absorption at higher temperature. The value of $\Delta H°$ provides information about the type of Pb(II) and Ni(II), absorption onto TNPs as follows [66]:

$$\Delta H° = 2.1–20.9 \text{ kJ mol}^{-1} \text{ (Physisorption)} \quad (13)$$

$$\Delta H° = 80–200 \text{ kJ mol}^{-1} \text{ (Chemisorption)} \quad (14)$$

The values of $\Delta H°$ are 9.012 and 12.772 kJ mol^{-1} for Pb(II) and Ni(II), respectively as shown in Table 6. This represents that that absorption of Pb(II) and Ni(II) ions onto TNPs, may be physical absorption process.

Table 6
Thermodynamic parameters of Pb(II) and Ni(II) adsorption onto TNPs at different temperatures.

Temperature (*K*)	Metal	$\ln K_0$	$\Delta G°$ (KJ mol^{-1})	$\Delta H°$ (KJ mol^{-1})	$\Delta S°$ (KJ mol^{-1} K^{-1})
303	Pb(II)	3.986	–10.041	9.012	0.063
313		4.074	–10.601		
323		4.228	–11.355		
333		4.292	–11.884		
303	Ni(II)	3.438	–8.661	12.772	0.071
313		3.612	–9.401		
323		3.758	–10.092		
333		3.897	–10.789		

Table 7
Desorption of Pb(II) and Ni(II) and from TNPs

Cycle	Metal	Adsorption		Desorption	
		C_i (mg L^{-1})	q_e (mg g^{-1})	C_f (mg L^{-1})	% desorption
1	Pb(II)	10	24.408	8.424	84.240
2		8.424	21.358	6.903	81.940
3		6.903	18.449	5.576	80.780
4		5.576	15.197	4.457	79.940
1	Ni(II)	10.00	19.317	8.660	86.60
2		8.660	17.900	7.396	85.400
3		7.396	16.711	6.234	84.300
4		6.234	14.088	5.218	83.700

3.9. Desorption and reusability

Desorption of metal ions from loaded absorbent and regeneration of the absorbent is a significant issue in view of reusability of the absorbent. For desorption studies, desorption experiments performed with Pb(II) and Ni(II), laden TNPs in 0.5 mol L^{-1} H_2SO_4 illustrated, that about 81.72% and 85.00% of the absorbed Pb(II) and Ni(II) was desorbed, respectively. Our findings also demonstrated that respective desorption of 84.24% and 86.60% for Pb(II) and Ni(II), occurred in the first round, respectively (Table 7). The removal of Pb(II) and Ni(II) did not reduce extraordinarily in the four consecutive cycles. The respective metal ions desorption efficiency of Pb(II) and Ni(II), onto TNPs was determined to be 84.24% and 86.60% in the first round, while in the second round demonstrated reduction difference of 2.30% and 1.20%, respectively. After the second round, a small reduction in the absorption ability of TNPs was found but the reduction was not much significant. This result suggests that the TNPs can be recycled for at least four times without losing much of its initial property.

4. Conclusions

In this study, a batch technique was used to examine the absorption of Pb(II) and Ni(II) from aqueous solutions onto TNPs as a function of different environment factors such as pH, IS, HA, contact time and temperature. The respective absorption of Pb(II) and Ni(II), increases with increasing pH values at pH < 5 and pH < 6, then sustains high level at pH 5.0–10.0 and pH > 6, respectively. The absorption of Pb(II) and Ni(II), dependents on ionic strength and foreign ions at pH < 6.0, whereas, no effect is observed at pH > 6.0. The presence of HA increases the Pb(II) and Ni(II), absorption into the TNPs at pH < 5.0 and pH < 6.0, whereas, the absorption reduced at pH > 6.0 and pH > 7.0, respectively. Furthermore, our results shows that ion exchange or outer-sphere surface complexation take place through the absorption of Pb(II) and Ni(II), onto TNPs at low pH values and inner-sphere surface complexation at high pH values. The thermodynamic parameters based on Langmuir model shows that the Pb(II) and Ni(II), absorption onto TNPs is spontaneous and endothermic in nature. The maximum absorption ability for Pb(II) and Ni(II), on the basis of Langmuir absorption equation was determined to be 40.00, 26.32 mg g^{-1}, respectively at 303 K, exhibiting higher efficiency for Pb(II) absorption than Ni(II) due to electronegativity and electrostatics differences. The values of enthalpy ($\Delta H°$) demonstrate that the absorption process is physical sorption. These findings indicates that TNPs is an appropriate absorbent for the absorption of Pb(II) and Ni(II), from aqueous solutions.

Acknowledgements

This work was supported by the National Natural Science Foundation of China (41571315) and CAS President's International Fellowship Initiative China (2017PCOO59)

Appendix A (Supplementary data)

Supplementary data associated with this article can be found, in the online version, at https://doi.org/10.5004/dwt.2019.23933

References

[1] E.-S.Z. El-Ashtoukhy, T.M. Zewail, N.K. Amin, Removal of heavy metal ions from aqueous solution by electrocoagulation using a horizontal expanded Al anode, Desal. Wat. Treat., 20 (2010) 72–79.

[2] P. Moradihamedani, K. Kalantari, A.H. Abdullah, N.A. Morad, High efficient removal of lead(II) and nickel(II) from aqueous solution by novel polysulfone/Fe3O4–talc nanocomposite mixed matrix membrane, Desal. Wat. Treat., 57 (2016) 28900–28909.

[3] S. Khan, Z. Dan, Y. Mengling, Y. Yang, H. Haiyan, J. Hao, Isotherms, kinetics and thermodynamic studies of adsorption of Ni and Cu by modification of Al2O3 nanoparticles with natural organic matter, Fullerenes Nanotubes. Carbon. Nanostruct., 26 (2018a) 158–167.

[4] A. Damaj, G.M. Ayoub, M. Al-Hindi, H. El Rassy, Activated carbon prepared from crushed pine needles used for the removal of Ni and Cd, Desal. Wat. Treat., 53 (2015) 3371–3380.

[5] G. Xuejun, Y. Zhe, D. Haiyang, G. Xiaohong, R. Qidong, L. Xiaofang, J. Xin, Simple combination of oxidants with zero-valent-iron (ZVI) achieved very rapid and highly efficient removal of heavy metals from water, Water. Res., 88 (2016) 671–680.

[6] S. Khan, Z. Dan, Y. Mengling, Y. Yang, H. Haiyan, J. Hao, Removal of Cd by humic acid modified TiO2 nanoparticles from aqueous solution, Desal. Wat. Treat., 100 (2017b) 193–203.

[7] M. Wu, T. Duan, Y. Chen, Q. Wen, Y. Wang, H. Xin, Surface modification of TiO2 nanotube arrays with metal copper particle for high efficient photocatalytic reduction of Cr(VI), Desal. Wat. Treat., 57 (2016) 10790–10801.

[8] A. Dabrowski, Z. Hubicki, P. Podkoscielny, E. Robens, Selective removal of the heavy metal ions from watersand industrial wastewaters by ion-exchange method, Chemosphere, 56 (2004) 91–106.

[9] K.Trivunac, S. Stevanovic, Removal of heavy metal ions from water by complexation assisted ultrafiltration, Chemosphere, 64 (2006) 486–491.

[10] X.K. Wang, C.L. Chen, J.Z. Du, X.L. Tan, D. Xu, S.M. Yu, Effect of pH and aging time on the kinetic dissociation of 243Am (III) from humic acid coated γ-Al2O3: a chelating resin exchange study, Environ. Sci. Technol., 39 (2005) 7084–7088.

[11] X.K. Wang, X. Zhou, J.Z. Du, W.P. Hu, C.L. Chen, Y.X. Chen, Using of chelating resin to study the kinetic desorption of Eu(III) from humic acid-Al2O3 colloid surfaces, Surf. Sci., 600 (2006) 478–483.

[12] M. Naushad, T. Ahamad, B.M. Al-Maswari, A.A. Alqadami, S.M. Alshehri, Nickel ferrite bearing nitrogen-doped mesoporous carbon as efficient adsorbent for the removal of highly toxic metal ion from aqueous medium, Chem. Eng. J., 330 (2017) 1351–1360.

[13] M. Naushad, Z.A. ALOthman, M.R. Awual, M.M. Alam, G.E. Eldesoky, Adsorption kinetics, isotherms and thermodynamic studies for the adsorption of Pb2+ and Hg2+ metal ions from aqueous medium using Ti(IV) iodovanadate cation exchanger, Ionics, 21 (2015) 2237–2245.

[14] M. Ghasemi, M. Naushad, N. Ghasemi, Y. Khosravi-Fard, Adsorption of Pb (II) from aqueous solution using new adsorbents prepared from agricultural waste: adsorption isotherm and kinetic studies, J. Ind. Eng. Chem., 20 (2014) 2193–2199.

[15] Y. Gutha, V.S. Munagapati, M. Naushad, K. Abburi, Removal of Ni(II) from aqueous solution by Lycopersicum esculentum (tomato) leaf powder as a low-cost biosorbent, Desal. Wat. Treat., 54 (2015) 200–208.

[16] M. Naushad, Z.A. ALOthman, Inamuddin, H. Javadian, Removal of Pb(II) from aqueous solution using ethylene diamine tetra acetic acid-Zr(IV) iodate composite cation exchanger: kinetics, isotherms and thermodynamic studies, J. Ind. Eng. Chem., 25 (2015) 35–41.

[17] M.K. Mondal, Removal of Pb (II) from aqueous solution by adsorption using activated tea waste, Korean. J. Chem. Eng., 27 (2010) 144–151.

[18] U.A. Guler, M. Sarioglu, Single and binary biosorption of Cu(II) and Ni(II) and methylene blue by raw and pretreated Spirogyra sp: equilibrium and kinetic modeling, J. Environ. Chem. Eng., 1 (2013) 369–377.

[19] T. Li, Y. Liu, Q. Peng, X. Hu, T. Liao, H. Wanga, M. Lu, Removal of lead (II) from aqueous solution with ethylenediamine-modified yeast biomass coated with magnetic chitosan microparticles: kinetic and equilibrium modeling, Chem. Eng. J., 214(2013) 189–197.

[20] C.H. Weng, Removal of nickel (II) from dilute aqueous solution by sluge ash, J. Environ. Eng., 128 (2002) 716–722.

[21] F. Banat, S. Al-Asheh, L. Al-Makhadmeh, Kinetics and equilibrium study of cadmium ion sorption onto date pits: an agricultural waste, Adsorpt. Sci. Technol., 20 (2002) 245–260.

[22] V.K. Gupta, M. Gupta, S. Sharma, Process development for the removal of lead and chromium from aqueous solution using red mud–an aluminum industry waste, Water. Res., 35 (2001) 1125–1134.

[23] A.A. Adesina, Industrial exploitation of photocatalysis progress, perspectives and prospects, Catal. Surv. Asia., 8 (2004) 265–273.

[24] N. Chitose, S. Ueta, T. Yamamoto, Radiolysis of aqueous phenol solutions with nanoparticles 1. phenol degradation and TOC removal in solutions containing TiO2 induced by UV, gamma-ray and electron beams, Chemosphere, 50 (2003) 1007–1013.

[25] K. Kabra, R. Chaudhary, R. Sawhney, Treatment of hazardous organic and inorganic compounds through aqueous-phase photocatalysis: a review, Ind. Eng. Chem. Res., 43 (2004) 7683–7696.

[26] P. Dutta, A. Ray, V. Sharma, J. Millero, Adsorption of arsenate and arsenite on titanium dioxide suspensions, J. Colloid. Interface. Sci., 278 (2004) 270–275.

[27] Z. Xu, X. Liu, Y. Ma, H. Gao, Interaction of nano-TiO2 with lysozyme: insights into the enzyme toxicity of nanosized particles, Environ. Sci. Pollut. Res., 17 (2010) 798–806.

[28] P. Umek, P. Cevc, A. Jesih, A. Gloter, C.P. Ewels, D. Arcon, Impact of structure and morphology on gas adsorption of titanate-based nanotubes and nanoribbons, Chem. Mater., 17 (2005) 5945–5950.

[29] C.K. Lee, C.C. Wang, L.C. Juang, M.D. Lyu, S.H. Hung, S.S. Liu, Effects of sodium content on the microstructures and basic dye cation exchange of titanate nanotubes, Colloids. Surf. A., 317 (2008) 164–173.

[30] H.Q. An, B.L. Zhu, H.Y. Wu, M. Zhang, S.R. Wang, S.M. Zhang, S.H. Wu, H. Weiping, Synthesis and characterization of titanate and CS2-modified titanate nanotubes as well as their adsorption capacities for heavy metal ions, Chem. J. Chin. U., 29 (2008) 439–444.

[31] S.S. Liu, C.K. Lee, H.C. Chen, C.C. Wang, L.C. Juang, Application of titanate nanotubes for Cu(II) ions adsorptive removal from aqueous solution, Chem. Eng. J., 147 (2009) 188–193.

[32] V. Belessi, G. Romanos, N. Boukos, D. Lambropoulou, C. Trapalis, Removal of Reactive Red 195 from aqueous solutions by adsorption on the surface of TiO2 nanoparticles, J. Hazard. Mater., 170 (2009) 836–844.

[33] M. Janus, E. Kusiak, J. Choina, J. Ziebro, A.W. Morawski, Enhanced adsorption of two azo dyes produced by carbon modification of TiO2, Desalination, 249 (2009) 359–363.

[34] D. Vu, Z. Li, H. Zhang, W. Wang, Z. Wang, X. Xu, B. Dong, C. Wang, Adsorption of Cu(II) from aqueous solution by anatase mesoporous TiO2 nanofibers prepared via electrospinning, J. Colloid. Interface. Sci., 367 (2012) 429–435.

[35] S. Khan, H. Şengül, Experimental investigation of stability and transport of TiO_2 nanoparticles in real soil columns, Desal. Wat. Treat., 57 (2016) 26196–26203.

[36] G. Yang, Z. Jiang, H. Shi, M.O. Jones, T. Xiao, P.P. Edwards, Z. Yan, Study on the photocatalysis of F–S co-doped TiO2 prepared using solvothermal method, Appl. Catal., B., 96 (2010) 458–465.

[37] J. Liu, R. Han, Y. Zhao, H. Wang, W. Lu, T. Yu, Y. Zhang, Enhanced photoactivity of V–N codoped TiO2 derived from a two-step hydrothermal procedure for the degradation of PCP–Na under visible light irradiation, J. Phys. Chem. C., 115 (2011) 4507–4515.
[38] F.A. Miller, C.H. Wilkins, Infrared spectra and characteristic frequencies of inorganic ions, Anal. Chem., 24 (1952) 1253–1294.
[39] S. Bakardjieva, V. ˇStengl, J. ˇSubrt, M.J. Dianez, M.J. Sayagues, Photoactivity of anatase-rutile TiO2 nanocrystalline mixtures obtained by heat treatment of homogeneously precipitated anatase, Appl. Catal., B., 58 (2005) 193–202.
[40] B. Hu, W. Cheng, H. Zhang, G. Sheng, Sorption of radionickel to goethite: effect of water quality parameters and temperature, J. Radioanal. Nucl. Chem., 285 (2010a) 389–398.
[41] X. Yang, S. Yang, S. Yang, J. Hu, X. Tan, X. Wang, Effect of pH, ionic strength and temperature on sorption of Pb(II) on NKF-6 zeolite studied by batch technique, Chem. Eng. J., 169 (2011) 86–93.
[42] M.A. Barakat, Adsorption behavior of copper and cyanide ions at TiO2–solution interface, J. Colloid. Interface. Sci., 291 (2005) 345–352.
[43] C.P. Huang, Y.S. Hsieh, S.W. Park, M.O. Corapcioglu, A.R. Bowers, H.A. Elliott, Metal Speciation, Separation and Recovery in: J.W. Paterson, R. Passino (Eds.), Ann Arbor Science Publisher, Novato, CA, 1986, pp. 437–465.
[44] Z. Jin, H. Gao, L. Hu, Removal of Pb(II) by nano-titanium oxide investigated by batch, XPS and model techniques, RSC. Adv., 5 (2015) 88520–88528.
[45] G. Sheng, S. Yang, J. Sheng, D. Zhao, X. Wang, Influence of solution chemistry on the removal of Ni(II) from aqueous solution to titanate nanotubes, Chem. Eng. J., 168 (2011) 178–182.
[46] C. Wu, C. Lin, P. Horng, Adsorption of copper and lead ions onto regenerated sludge from a water treatment plant, J. Environ. Sci. Health. A., 39 (2004) 237–252.
[47] S.W. Wang, J. Hu, J.X. Li, Y.H. Dong, Influence of pH, soil humic/fulvic acid, ionic strength, foreign ions and addition sequences on sorption of Pb(II) onto GMZ bentonite, J. Hazard. Mater., 167 (2009) 44–51.
[48] J.X. Li, J. Hu, G.D. Sheng, G.X. Zhao, Q. Huang, Effect of pH, ionic strength, foreign ions and temperature on the sorption of Cu(II) from aqueous solution to GMZ bentonite, Colloid. Surf. A., 349 (2009) 195–201.
[49] B. Hu, W. Cheng, H. Zhang, S. Yang, Solution chemistry effects on sorption behavior of radionuclide 63Ni(II) in illite-water suspensions, J. Nucl. Mater., 406 (2010b) 263–270.
[50] Q.H. Fan, D.D. Shao, J. Hu, W.S. Wu, X.K. Wang, Comparison of Ni2+ sorption to bare and ACT-graft attapulgites: effect of pH, temperature and foreign ions, Surf. Sci., 602 (2008) 778–785.
[51] Y.B. Sun, C.L. Chen, J.D.D. Shao, X. Li, X.L. Tan, G.X. Zhao, S.B. Yang, X.K. Wang, Enhanced adsorption of ionizable aromatic compounds on humic acid-coated carbonaceous adsorbents, RSC. Adv., 2 (2012) 10359–10364.
[52] Y.B. Sun, S.B. Yang, G.X. Zhao, Q. Wang, X.K. Wang, Adsorption of polycyclic aromatic hydrocarbons on graphene oxides and reduced graphene oxides, Chem.–Asian. J., 8 (2013) 2755–2761.
[53] S. Ghosh, H. Mashayekhi, B. Pan, P. Bhowmik, B. Xing, Colloidal behavior of aluminum oxide nanoparticles as affected by pH and natural organic matter, Langmuir, 24 (2008) 12385–12391.
[54] K. Yang, B. Xing, Adsorption of fulvic acid by carbon nanotubes from water, Environ. Pollut., 157 (2009) 1095–1100.
[55] A.S. Poursani, A. Nilchi, A.H. Hassani, A novel method for synthesis of nano-γ-Al2O3: study of adsorption behavior of chromium, nickel, cadmium and lead ions, Int. J. Environ. Sci. Technol., 12 (2015) 2003–2014.
[56] R. Bushra, M. Naushad, R. Adnan, Z.A. ALOthman, M. Rafatullah, Polyaniline supported nanocomposite cation exchanger: synthesis, characterization and applications for the efficient removal of Pb2+ ion from aqueous medium, J. Ind. Eng. Chem., 21 (2015) 1112–1118.
[57] M. Ghasemi, M. Naushad, N. Ghasemi, Y. Khosravi-fard, A novel agricultural waste based adsorbent for the removal of Pb(II) from aqueous solution: kinetics, equilibrium and thermodynamic studies, J. Ind. Eng. Chem., 20 (2014) 454–461.
[58] M.R. Awual, G.E. Eldesoky, T. Yaita, M. Naushad, H. Shiwaku, Z.A. AlOthman, S. Suzuki, Schiff based ligand containing nano-composite adsorbent for optical copper(II) ions removal from aqueous solutions, Chem. Eng. J., 279 (2015) 639–647.
[59] M. Naushad, Surfactant assisted nano-composite cation exchanger: development, characterization and applications for the removal of toxic Pb2+ from aqueous medium, Chem. Eng. J., 235 (2014) 100–108.
[60] T. Phuengprasop, J. Sittiwong, F. Unob, Removal of heavymetals ions by iron oxide coated sewage sludge, J. Hazard. Mater., 186 (2011) 502–507.
[61] X.Y. Guo, S.Z. Zhang, X.Q. Shan, Adsorption of metal ions on lignin, J. Hazard. Mater., 15 (2008) 134–142.
[62] A. Hammaini, F. Gonzalez, A. Ballester, M.L. Blázquez, J.A. Muñoz, Biosorption of heavy metals by activated sludge and their desorption characteristics, J. Environ. Manage., 84 (2007) 419–426.
[63] E. Malkoc, Y. Nuhoglu, Ni (II) removal from aqueous solution using tea factory waste, J. Hazard. Mater., 127 (2005) 120–128.
[64] E. Malkoc, Y. Nuhoglu, Ni (II) removal from aqueous solutions using cone biomass of thuja orientalis, J. Hazard. Mater., 137 (2006) 899–908.
[65] S. Mahdavi, M. Jalali, A. Afkhami, Heavy metals removal from aqueous solutions by Al2O3 nanoparticles modified with natural and chemical modifiers, Clean. Technol. Environ. Policy., 17 (2015) 85–102.
[66] Y. Liu, Y.J. Liu, Biosorption isotherms, kinetics and thermodynamics, Sep. Purif. Technol., 61 (2008) 229–242.
[67] A.A. Khan, R.P. Singh, Adsorption thermodynamics of carbofuran on Sn (IV) arsenosilicate in H+, Na+ and Ca2+ forms, Colloids. Surf., 24 (1987) 33–42.

Supplementary data

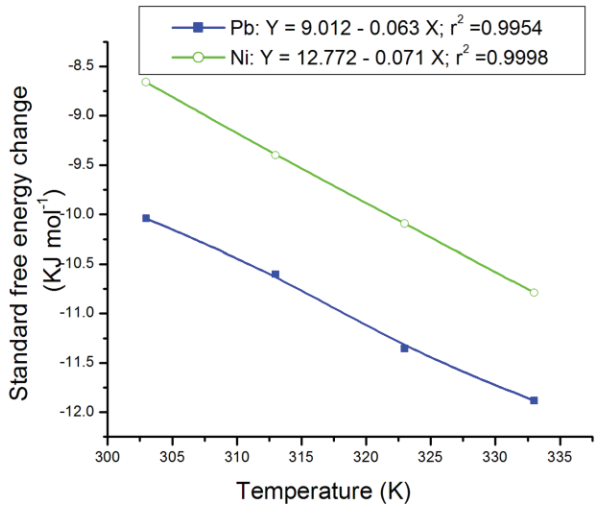

Fig. S1. Polt of standard free energy change (ΔG°) vs. temperature (K) for thermodynamic parameters of Pb(II) and Ni(II) adsorption onto TNPs.